Multiple determinants in voltage-dependent P/Q calcium channels control their retention in the endoplasmic reticulum

Veronique Cornet, Delphine Bichet, Guillaume Sandoz, Isabelle Marty, Jacques Brocard, Emmanuel Bourinet, Yasuo Mori, Michel Villaz, Michel de Waard

European Journal of Neuroscience, Vol. 16, pp. 883–895, 2002

Multiple determinants in voltage-dependent P/Q calcium channels control their retention in the endoplasmic reticulum

Véronique Cornet,[1*] Delphine Bichet,[2*] Guillaume Sandoz,[2] Isabelle Marty,[2] Jacques Brocard,[2] Emmanuel Bourinet,[3] Yasuo Mori,[4] Michel Villaz[2] and Michel De Waard[2]
[1]INSERM U464, Laboratoire de Neurobiologie des Canaux Ioniques, Faculté de Médecine Nord, Boulevard Pierre Dramard, 13916 Marseille Cedex 20, France
[2]INSERM EMI 9931, Laboratoire Canaux Ioniques Signalisation, CEA, DBMS, 17, Rue des Martyrs, 38054 Grenoble Cedex 9, France.
[3]Physiopathologie des Canaux Ioniques, IGH CNRS UPR1142, 141 Rue de la Cardonille, 34396 Montpellier Cedex 5, France
[4]Department of Information Physiology, National Institute of Physiological Sciences, Okazaki 444 Aichi, Japan.

Keywords: calcium channel, CD8, ER retention, trafficking.

Abstract

Surface expression level of voltage-dependent calcium channels is tightly controlled in neurons to avoid the resulting cell toxicity generally associated with excessive calcium entry. Cell surface expression of high voltage-activated calcium channels requires the association of the pore-forming subunit, $Ca_v\alpha$, with the auxiliary subunit, $Ca_v\beta$. In the absence of this auxiliary subunit, $Ca_v\alpha$ is retained in the endoplasmic reticulum (ER) through mechanisms that are still poorly understood. Here, we have investigated, by a quantitative method based on the use of CD8α chimeras, the molecular determinants of $Ca_v\alpha_{2.1}$ that are responsible for the retention, in the absence of auxiliary subunits, of P/Q calcium channels in the ER (referred to here as 'ER retention'). This study demonstrates that the I–II loop of $Ca_v\alpha_{2.1}$ contains multiple ER-retention determinants beside the β subunit association domain. In addition, the I–II loop is not the sole domain of calcium channel retention as two regions identified for their ability to interact with the I–II loop, the N- and C-termini of $Ca_v\alpha_{2.1}$, also produce ER retention. It is also not an obligatory determinant as, similarly to low-threshold calcium channels, the I–II loop of $Ca_v\alpha_{1.1}$ does not produce ER retention in COS7 cells. The data presented here suggests that ER retention is suppressed by sequential molecular events that include: (i) a correct folding of $Ca_v\alpha$ in order to mask several internal ER-retention determinants and (ii) the association of other proteins, including the $Ca_v\beta$ subunit, to suppress the remaining ER-retention determinants.

Introduction

High voltage activated calcium channels are multimeric proteins composed of the main pore-forming subunit, $Ca_v\alpha$, and at least two auxiliary subunits, $Ca_v\beta$ and $Ca_v\alpha_2\delta$ (Flockerzi *et al.*, 1986; Witcher *et al.*, 1993). Molecular diversity in calcium channels is introduced by gene multiplicity. At least 10 genes code for $Ca_v\alpha$, four for $Ca_v\beta$ and three for $Ca_v\alpha_2\delta$ (Ertel *et al.*, 2000). Promiscuity in subunit interaction and alternative splicing of these genes represent two additional mechanisms for introducing structural and functional diversity (Liu *et al.*, 1996; Scott *et al.*, 1996; Reimer *et al.*, 2000). Such a molecular diversity is required to support the cellular functions in which these channels are involved, e.g. muscle contraction, cellular excitability, gene expression, metabolism or neurotransmitter release. For instance, both N- and P/Q-type channels appear to be involved in neurotransmitter release through direct molecular interactions with SNARE proteins such as SNAP-25, syntaxin and synaptotagmin. Additionally, P/Q calcium channels seem to control the transcription level of syntaxin, a synaptic vesicle constituent protein (Sutton *et al.*, 1999).

The implication of each calcium channel type in a specific cellular function requires a very tight control of their surface expression level by the cell. This is best demonstrated for high-threshold voltage-dependent calcium channel expression which is strictly controlled by the association of the main pore-forming subunit, $Ca_v\alpha$, with its auxiliary $Ca_v\beta$ subunits (Brice *et al.*, 1997; Bichet *et al.*, 2000). In the absence of this subunit, these calcium channels remain strictly confined to the endoplasmic reticulum (ER). This has further been confirmed through several heterologous expression experiments in which it was demonstrated that $Ca_v\beta$ subunits greatly improve the expression level of $Ca_v\alpha$. The $Ca_v\alpha_2\delta$ subunits appear to play a similar role though this effect requires the presence of the $Ca_v\beta$ subunit to manifest itself (Walker & De Waard, 1998). Curiously, the facilitating effect of the $Ca_v\beta$ protein on $Ca_v\alpha$ cell surface expression appears to be limited in amplitude in spite of a clear excess molar level in favour of the auxiliary subunit. This observation points to the existence of several other factors controlling the expression level of $Ca_v\alpha$ at the surface of the cells. As recent observations point out that calcium channels are macromolecular complexes that include structural and regulatory components (Davare *et al.*, 2001), it is tempting

Correspondence: Dr Michel De Waard, as above. E-mail: mdewaard@cea.fr

*V.C. and D.B. contributed equally to this work

Received 7 February 2002, revised 27 May 2002, accepted 3 July 2002

doi:10.1046/j.1460-9568.2002.02168.x

to envision that other proteins, beside the constituent $Ca_v\beta$ subunit, may control the targeted expression of voltage-dependent calcium channels in specialized compartments of the cell surface.

Here, it was investigated whether $Ca_v\alpha$ subunits may contain ER-retention determinants other than the previously identified $Ca_v\beta$-dependent I–II loop domain (Bichet *et al.*, 2000). The data presented here point to the existence of multiple ER-retention determinants both within and outside the I–II loop. Several of the regions identified appear able to interact with each other suggesting that appropriate folding would represent a first essential preliminary step in overcoming ER retention.

Materials and methods

Materials, including antibodies and peptides

For quantification experiments by ELISA, we used a mouse biotinylated antihuman CD8 monoclonal antibody from Calbiochem (Lot B30879). Monoclonal (HIT8a) and polyclonal (H-160) antihuman CD8 antibodies (Pharmingen and Santa-Cruz) were used for immunocytochemistry on nonpermeabilized and permeabilized COS7 cells, respectively. The monoclonal anti-BiP antibody directed against the carboxyl-terminus of rat BiP (10C3) is from StressGen Biotechnologies, San Diego, USA. Donkey antimouse conjugated to Texas Red (DAM-TxR) or FITC (DAM-FITC) and donkey antirabbit conjugated to Texas Red (DAR-TxR) or FITC (DAR-FITC) were from Jackson Immunoresearch Laboratories (Immunotech, France). Neutravidin-horse radish peroxidase (–HRP) was from PerBio (France).

Plasmid constructions

Chimera CD8 constructs were made as previously described (Bichet *et al.*, 2000; Geib *et al.*, 2002). Briefly, cDNA sequences derived from rabbit $Ca_v\alpha_{1.1}$ (GenBank accession N° M23919), rabbit $Ca_v\alpha_{1.2}$ (N° M57974), $Ca_v\alpha_{2.1}$ (N° X57477), rabbit $Ca_v\alpha_{2.2}$ (N° D14157), rabbit $Ca_v\alpha_{2.3}$ (N° X67856) and rat $Ca_v\alpha_{3.1}$ (N° AF027984) were amplified by PCR with forward and reverse oligonucleotides containing *Eco*RI and *Bam*HI sites, respectively. The PCR products were then cut with these restriction enzymes and incorporated between the CD8 sequence (without its cytoplasmic part) and the myc tag of the pcDNA3-CD8-myc plasmid. Site-directed mutagenesis in the I–II loop of $Ca_v\alpha_{2.1}$ was performed using the Quick-Change™ Site-Directed Mutagenesis Kit (Stratagene). All constructs were checked by restriction site mapping and sequencing. The CD8-stop construct was as previously described (Bichet *et al.*, 2000).

In vitro *translation and binding experiments*

[^{35}S]-methionine-labelled proteins were obtained by coupled *in vitro* transcription and translation using the TNT™ system of Promega. Translated proteins were loaded and separated onto 3–12% gels, which were subsequently dried and exposed for autoradiography. GST fusion proteins were purified as previously reported (De Waard *et al.*, 1995). Purified GST fusion proteins were coupled to glutathione-agarose beads by a 30-min incubation in buffer A: TBS (25 mM Tris, 150 mM NaCl [pH 7.4]), 0.1% Triton X-100. Residual unbound fusion proteins were removed by a first wash with buffer A. Binding of [^{35}S]-I–II$_{2.1}$ loop was initiated by the addition of 1–2 μL of the translation product in 0.5 mL volume of beads/buffer A (1–5 pM of [^{35}S]-I–II$_{2.1}$). Estimated fusion protein concentration was 1 μM. The mixture was incubated overnight at 4 °C. Beads were then washed 4 × with 1 mL buffer A, and the bound radioactive protein analysed by SDS-PAGE and autoradiography. Non-specific binding was determined as the radioactivity associated to GST-glutathione-agarose beads.

Cell cultures and transfection

COS7 cells were maintained in Dulbecco's modified Eagles medium (DMEM glutamax, Invitrogen) containing 10% fetal bovine serum and 100 μg/mL penicillin/streptomycin at 37 °C in 5% CO_2. Transfections were performed using the FuGENE™6 reagent (ROCHE diagnostic). For 18-mm-diameter coverslips (immunocytochemistry), 0.5 μg cDNA in FuGENE mix (1.5 μL FuGENE and 25 μL of DMEM) were incubated for 20 min at room temperature and the mixture was added to the cell culture. Cells were left in the presence of the transfection media for ~24 h. For 35-mm-diameter plastic dishes (for ELISA quantification), we followed the same procedure except that the cDNA/FuGENE quantity was increased 4-fold.

Immunocytochemistry

For cell surface and intracellular labelling of chimera CD8 proteins, 24 h-transfected-COS7 cells were washed twice with DMEM and incubated for 45 min at 4 °C with the mouse monoclonal anti-CD8 antibody (20 μg/mL) in DMEM, 10 mM HEPES, and 0.1% bovine serum albumin (BSA) (pH 7.4 with NaOH). This first antibody treatment allows the cell surface labelling of CD8 proteins. Cells were then washed 3 × with phosphate-buffered saline (PBS) supplemented with 1 mM $CaCl_2$ and 1 mM $MgCl_2$ at pH 7.4, fixed with 4% paraformaldehyde in 0.1 M phosphate buffer (PB) for 20 min at room temperature, rinsed 3 × with PB buffer, and incubated for 10 min in 50 mM NH_4Cl in PB. Next, the cells were permeabilized for 30 min with PB supplemented with 0.06% saponin and 0.2% gelatin (buffer A), and incubated at room temperature for 45 min with the rabbit polyclonal anti-CD8 antibody (1 : 500) in buffer A. This incubation labelled the intracellular pool of chimera CD8 proteins. Following three washes with buffer A, the cells were incubated 45 min in buffer A with a mixture of secondary antibodies (1 : 400 dilution of DAM-TxR for cell surface labelling and DAR-FITC for intracellular labelling of CD8 chimeras). After three washes in buffer A, coverslip preparations were mounted in Mowiol (Aldrich, France) and observed with a confocal microscope.

For intracellular coimmunostaining of chimera CD8 proteins and BiP, the ER resident protein, transfected COS7 cells were washed 3 × in PBS supplemented with 1 mM $CaCl_2$ and 1 mM $MgCl_2$ at pH 7.4, fixed with 4% paraformaldehyde in 0.1 M phosphate buffer (PB) for 20 min at room temperature, rinsed 3 × with PB buffer, and incubated for 10 min in 50 mM NH_4Cl in PB. Next, the cells were permeabilized for 30 min with buffer A, and incubated at room temperature for 45 min with a mixture of rabbit polyclonal anti-CD8 antibody (1 : 500) and mouse monoclonal anti-BiP (10 μg/mL) in buffer A. Cells were then washed 3 × with buffer A, and incubated for 45 min in buffer A with a mixture of secondary antibodies (dilution of 1 : 400 of DAM-FITC for BiP staining and DAR-TxR for CD8 chimera proteins). After three washes in buffer A, the coverslip preparations were mounted in Mowiol and observed with a confocal microscope.

Quantification of plasma membrane expression level of CD8 chimera by ELISA

COS7 cells were grown to confluence, transfected with one of the CD8 chimera constructs for 24 h, and the various cell expression levels of CD8 chimera proteins were obtained by one of the two following treatments. For the quantification of total cell expression level, COS7 cells were washed twice with PBS, fixed for 5 min with

paraformaldehyde 1% in PB, washed 3 × with PBS, incubated 10 min with 50 mM NH_4Cl in PB, and rinsed 3 × with PBS. Next, cells were incubated for 1 h at room temperature in permeabilizing conditions with a mouse biotinylated antihuman CD8 monoclonal antibody (3 μg/mL; anti-CD8-biot) in buffer A (total cell labelling of CD8 chimera proteins). Cells were then washed 3 × with PBS before undergoing the ELISA quantification procedure. For the quantification of cell surface expression level, COS7 cells were washed twice with ice-cold DMEM, incubated 1 h at 4 °C with anti-CD8-biot (3 μg/mL) in DMEM supplemented with 20 mM HEPES, pH 7.2 and 0.1% BSA. Cold temperatures were used to avoid internalization of the immune complex. To be in similar experimental conditions as for the quantification of total cell expression level of CD8 chimera proteins, these cells were also fixed with paraformaldehyde and incubated with PB/NH_4Cl. Cells were then washed with PBS before undergoing the same ELISA quantification procedure as for total cell expression level evaluation.

For the ELISA quantification procedure, cells were scrapped off the bottom of the Petri dishes, transferred to Eppendorf tubes, and centrifuged at 4 °C for 10 min at 10 000 r.p.m. (Jouan MR22, Rotor AM2-19). The cell pellet was resuspended and lysed with 300 μL of buffer B (50 mM NaCl, 10 mM Tris/HCl, pH 7.4, 1% Triton X-100, 0.1% SDS, 0.1% BSA). The lysates were separated into three pools of 100 μL (each individual fraction representing one point of a triplicate value) and added for 3 h at 37 °C to individual wells of EIA/RIA plates (Costar) that were precoated with secondary GAM immunoglobulin G. Pre-coating of the wells was performed by adding 200 μL of 10 μg/mL of GAM immunoglobulin G in 50 mM $NaHCO_3$, pH 9.0 for 3 h at 37 °C, followed by two washes with PBS and a saturation of nonspecific sites with buffer B incubation (1 h at 37 °C). The concentration of GAM immunoglobulin G used to precoat the wells is saturating (data not shown). Following incubation with the cell lysates, the wells were washed several times in various conditions: three washes with PBS, one incubation of 5 min with buffer B and three washes with PBS. Next, 100 μL of 1 μg/mL neutravidine-HRP in buffer B was added to each well and incubated 1 h at room temperature. Again, three washes of the wells were performed with PBS, followed by a 5-min incubation with PB and three washes with PBS. HRP activity was detected by a colourimetric reaction induced by the addition of 0.4 mg/mL *o*-phenylenediamine in 25 mM Na-citrate, 50 mM Na_2PO_4, pH 5.0 supplemented with 0.01% H_2O_2. After 5 min, the colourimetric reaction is stopped with 50 μL of 2 M H_2SO_4. Optical density (OD) was determined at 490 nm.

Data analysis leading to the determination of cell surface expression efficiencies of CD8 chimera proteins

For each experimental condition, the nonspecific OD values (cell surface and total cell), corresponding to nontransfected COS7 cells, were subtracted from the surface and total cell OD values derived from the expression of wild-type or chimera CD8 proteins in COS7 cells, these specific values were called OD_S and OD_T for cell surface and total cell values, respectively. For permeabilized and non-permeabilized cells, non-specific OD values represented 9.5 ± 3.8% (n = 12) and 7.5 ± 4.4% (n = 12) of OD values obtained upon transfection of wild-type CD8-stop protein, respectively. To obtain the cell surface expression efficiency (SEE) of each expressed protein, we calculated the ratio OD_S/OD_T and expressed it in percentage. SEE values obtained for each CD8 chimera protein was systematically compared to the SEE value obtained for CD8-stop in the same experiment.

Electrophysiological recordings

Xenopus laevis stage V or VI oocytes were microinjected with 50 nL of various cRNA mixtures (0.3 μg/μL wild-type $Ca_v\alpha_{2.1}$ ± 0.1 μg/μL of each chimera CD8). Cells were then incubated for 6–8 days in defined nutrient oocyte medium (Eppig & Dumont, 1976) prior to recording. For Ba^{2+} current recordings, two-electrode voltage-clamping was performed with a GeneClamp amplifier (Axon Instruments, Foster City, CA). The extracellular recording solution contained (in mM): $Ba(OH)_2$ 40, NaOH 50, KCl 3, HEPES 5, niflumic acid 1, pH 7.4 with methane sulphonic acid. Electrodes filled with (in mM): KCl 140, EGTA 10 and HEPES 10 (pH 7.2 with KOH) had resistances comprised between 0.5 and 1 MΩ. Current records were filtered on-line at 2 kHz, leak subtracted by a P/4 protocol, and sampled at 5–10 kHz. Data were analysed using pCLAMP version 6.03 (Axon Instruments).

Results

Studying cell surface expression level of voltage-dependent calcium channels by biochemical techniques is an extremely difficult task owing to the large size of these proteins. Besides, many cell regulatory mechanisms come into play to limit the number of these structures at the plasma membrane because of the well-known cell toxicity produced by excessive calcium influx. To circumvent these problems, this study used another approach to the study of calcium channel expression level by incorporating partial cDNA sequences of the pore-forming subunit, $Ca_v\alpha$, into a reporter construct, here the α chain of the human CD8 molecule in which the sequence coding for its cytoplasmic part had been removed. Using CD8-$Ca_v\alpha$ chimera constructs instead of full-length $Ca_v\alpha$ also presents the advantage that it is expressed at higher protein levels than the calcium channel itself. Part of this higher expression level is due to the size of the constructs used but also to a simplified membrane topology of the resulting proteins (a single transmembrane segment instead of 24). Finally, it should be emphasized that the chimera proteins do not permeate calcium into the cell by themselves (data not shown).

Figure 1A presents a schematic diagram illustrating the chimera strategy used to subclone various $Ca_v\alpha_{2.1}$ cDNA sequences. The CD8-stop construct that is used as a control for the study of cell surface expression efficacy contains not only the ectodomain and the transmembrane segment of $CD8_\alpha$, but also a myc tag at the intracellular part. Antibodies are available towards the ectodomain and the myc sequence making this type of construct very useful for immunocytochemistry and for a quantitative analysis of protein expression level. The aim of this study was to investigate the cell surface expression efficiency of various CD8 chimera proteins in COS7 cells, using a quantitative method derived from an ELISA principle. This method is extensively described in the 'Materials and methods' section. Briefly, it is based on the determination of the quantity of mouse anti-CD8-biot antibody that binds to the GAM immunoglobulin G immobilized in the wells of the ELISA plate. The quantity of anti-CD8-biot antibody bound is determined through the use of a neutravidine-HRP colourimetric reaction. This quantification of the anti-CD8-biot antibody is itself an index of the total quantity of CD8 proteins recognized by this antibody. It was found that the technique is extremely reliable if several experimental parameters are controlled. The first one is that variation in the quantity of anti-CD8-biot antibody bound onto the GAM immunoglobulin G of the wells must be in the detectable range. Figure 1B shows that concentrations of anti-CD8-biot antibodies above 10 ng/well saturate the binding capacity of GAM immunoglobulins. In this assay, the maximal OD

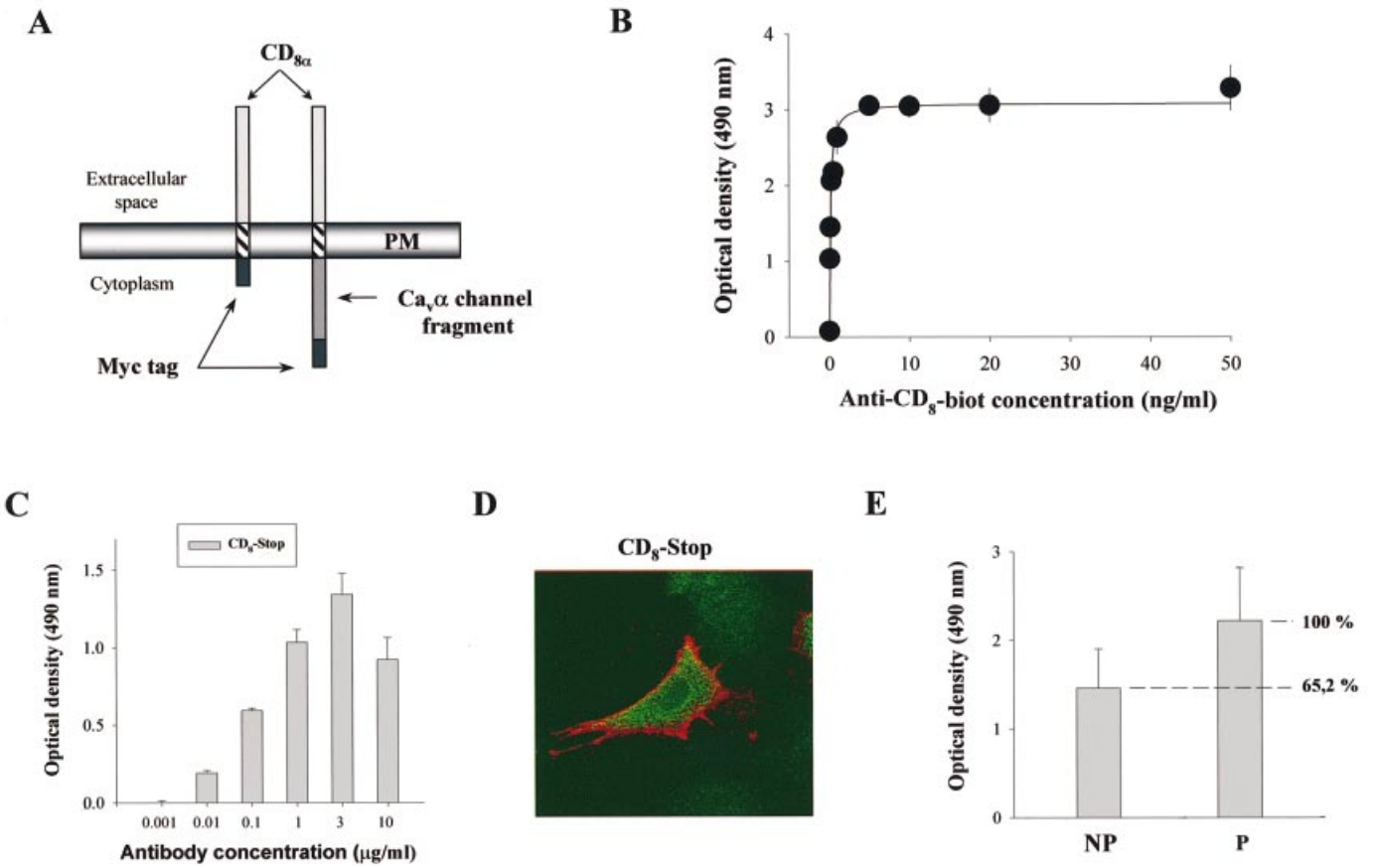

FIG. 1. A quantitative approach to CD8 cell surface expression in COS7 cells. (A) Schematic representation of CD8 chimeric proteins. The ectodomain and the transmembrane domain of CD8 were conserved, whereas the cytoplasmic domain was replaced by a myc tag or $Ca_v\alpha$ calcium channel fragments coupled to myc. (B) Various concentrations of anti-CD8 antibody coupled to biotin were tested to saturate antimouse antibody coated onto ELISA 96 wells. Neutravidin-HRP signals were then detected by an optical density measurement at 490 nm. (C) Various anti-CD8 antibody concentrations were used to detect CD8-stop-myc expression in COS7 cells. The specific signal was subtracted from the signal obtained in untransfected cells. Maximal detection was observed at an antibody concentration close to 3 μg/mL. (D) Confocal image illustrating the cell surface expression of CD8-stop-myc (red labelling, nonpermeabilized COS7 cell), superimposed with the total expression of the protein (green labelling, following permeabilization of the same cell). See Methods. (E) CD8-stop-myc membrane expression was determined using 3 μg/mL anti-CD8 antibody in nonpermeabilized and permeabilized conditions. The optical density obtained in permeabilized conditions corresponds to total CD8-stop-myc expression in COS7 and is considered as the 100% value. The ratio between cell surface (NP, non permeabilized) and total (P, permeabilized) expression corresponds to the percentage of cell surface expression of CD8-stop-myc (here, 65.2%) and is termed SEE level throughout the text.

value that can theoretically be reached by binding of anti-CD8-biot antibody to GAM immunoglobulin G is close to 3. Therefore, OD values measured for CD8 protein expression in COS7 cells should be below the maximal OD values detected in the standard curve. Such standard curves were realized for each experiment, though very little variability was seen in maximal OD values (between 2.77 and 3.60 with a mean value of 3.01 ± 0.39, $n = 12$). A second aim was to use a saturating anti-CD8-biot antibody concentration to optimize the detection of CD8 proteins expressed in the COS7 cells. Figure 1C illustrates an experiment in which various anti-CD8-biot antibody concentrations (from 1 ng/mL to 10 μg/mL) were incubated with permeabilized COS7 cells expressing the CD8-stop protein. Following the procedure described in the 'Materials and methods' section (cell scraping, solubilization and ELISA quantification), increasing OD values were measured that saturated at ~3 μg/mL of anti-CD8-biot antibody concentration. Of note, the maximal OD value reached (1.81 ± 0.13; total average of triplicate values without nonspecific subtraction) with 3 μg/mL anti-CD8-biot antibody was below the saturating value of the system (OD of 2.77 ± 0.02) which validates the saturation curve described in Fig. 1B. Also, non-specific values (untransfected COS7 cells) represented on average 9.5 ± 3.8% ($n = 12$) of the total OD values observed for CD8-stop transfected cells. Next, the cell surface expression efficiency (SEE) of our control protein was evaluated allowing it to be used as a comparative reference for the expression of chimera CD8 proteins. Figure 1D illustrates the expression of CD8-stop in a COS7 cell, stained first with a monoclonal anti-CD8 in nonpermeabilized conditions, and a second time with a polyclonal anti-CD8 after permeabilization. This example demonstrates that CD8-stop protein is not perfectly distributed at the plasma membrane of COS7 cells; a significant proportion of the protein remaining localized inside of the cell. This may simply reflect continuous protein synthesis and/or cell trafficking of neosynthesized proteins. The next step in the study therefore, was the evaluation of the relative proportion of CD8-stop expression in the plasma membrane vs. total expression, using the ELISA quantification method described above. The results obtained (Fig. 1E) demonstrate that, with SEE = 65.2 ± 7.1% ($n = 12$), CD8-stop expression level is on average high at the plasma membrane. This proportion was relatively stable with average triplicate SEE values ranging between 50.6 and 74.9%, the two extreme values

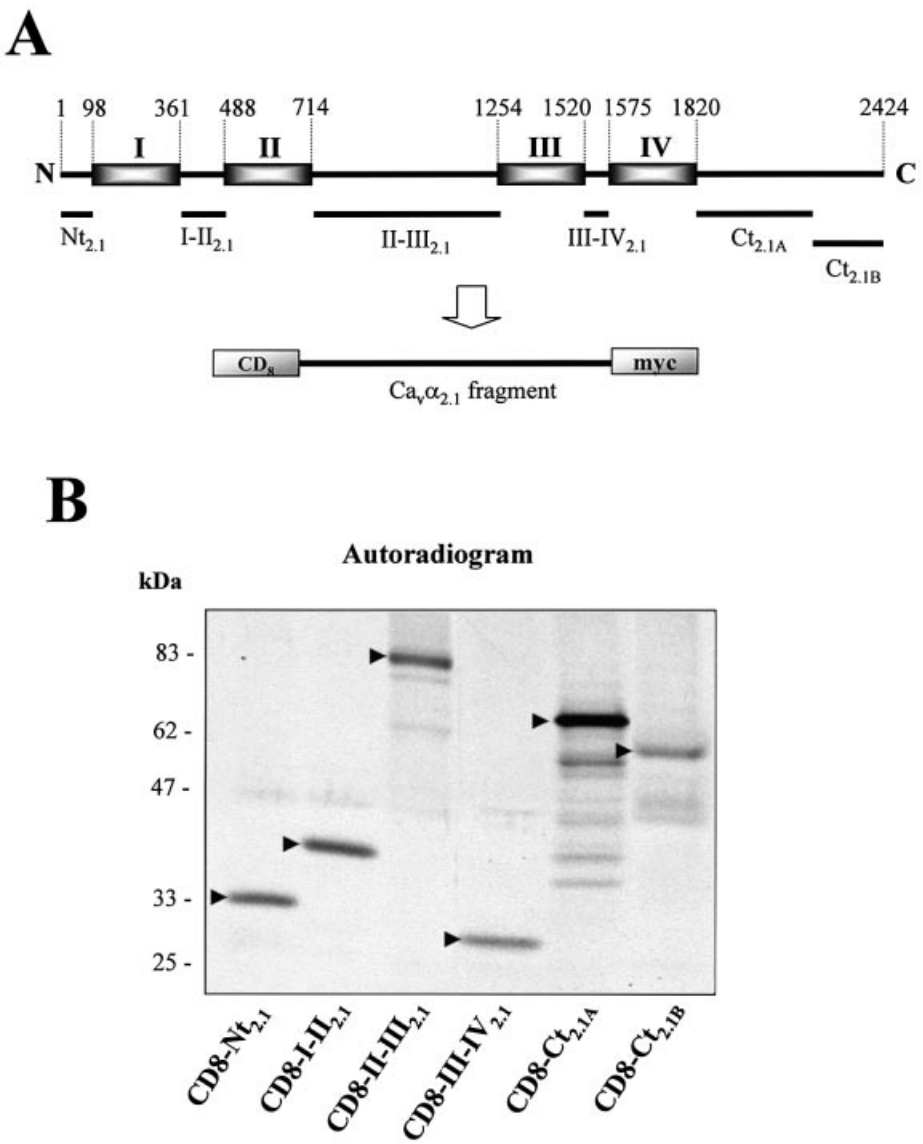

FIG. 2. CD8 chimeric proteins of $Ca_v\alpha_{2.1}$ (A) Schematic diagram of $Ca_v\alpha_{2.1}$. Amino acid positions are shown above, transmembrane domains are shown as dark boxes and numbered I to IV. Bottom, cytoplasmic sequences of $Ca_v\alpha_{2.1}$ fused to $CD8_\alpha$. (B) Autoradiogram of *in vitro* translated chimeric proteins separated on a 9–15% gradient SDS-PAGE. The observed molecular weights of the chimeric proteins are in the expected range (see arrows for full-length proteins). Additional bands visible in each lane result from proteolytic degradation and/or incomplete protein synthesis.

observed in our experiments. It should be noted that with this ELISA ratio quantification method, SEE levels should be independent of total expression levels in cells, thereby facilitating comparative analysis between various proteins.

In our laboratory, Bichet *et al.* (2000) described the role of the I–II loop of $Ca_v2.1$ in ER retention in COS7 cells, and we are extending these observations to other major cytoplasmic sequences of the $Ca_v\alpha_{2.1}$ channel. Figure 2A illustrates the various CD8 chimera constructs made with the rabbit $Ca_v\alpha_{2.1}$ cDNA sequence (Mori *et al.*, 1991). These constructs were checked by sequencing and also by *in vitro* translation. An autoradiogram of a 9–15% gradient SDS-PAGE shows that the actual sizes of the full-length *in vitro* translated products are in agreement with the expected sizes (Fig. 2B). Next, the cell surface (nonpermeabilized, NP) and intracellular (permeabilized, P) expression of the chimera CD8-$Ca_v\alpha_{2.1}$ proteins was examined in COS7 cells (Fig. 3A), for comparison, the expression of CD8-stop is shown in Fig. 1D. It was found that, like CD8-I–$II_{2.1}$, there was no cell surface expression of chimeras CD8-$Nt_{2.1}$, CD8-$Ct_{2.1A}$ and CD8-$Ct_{2.1B}$ suggesting that these proteins were retained somewhere in the cell along the trafficking pathway. $Ct_{2.1A}$ and $Ct_{2.1B}$ are slightly overlapping sequences of the carboxyl-terminus of $Ca_v\alpha_{2.1}$. In contrast to these three CD8-$Ca_v\alpha_{2.1}$ chimera proteins, the two other chimera proteins, CD8-II–$III_{2.1}$ and CD8-III–$IV_{2.1}$, presented clearly detectable expression levels at the cell surface. These results suggest that, for $Ca_v\alpha_{2.1}$ at least, there are three cytoplasmic sequences that restrict plasma membrane expression of the channel in COS7 cells: the amino- and carboxyl termini and the I–II loop. These immunofluorescence findings were confirmed and quantified by the ELISA method (Fig. 3B). As previously shown, 65.2 ± 7.1% (n = 12) of CD8-stop protein is expressed at the plasma membrane

(Fig. 1E). In order to compare between different experiments in which the cell surface expression efficiency of CD8-stop was slightly variable (between 50.6 and 74.9%), the cell surface expression efficiency of chimeric CD8-$Ca_v\alpha_{2.1}$ proteins was normalized to the average value obtained for CD8-stop in the same experiment. The cell surface expression of CD8-stop is therefore referred to as the

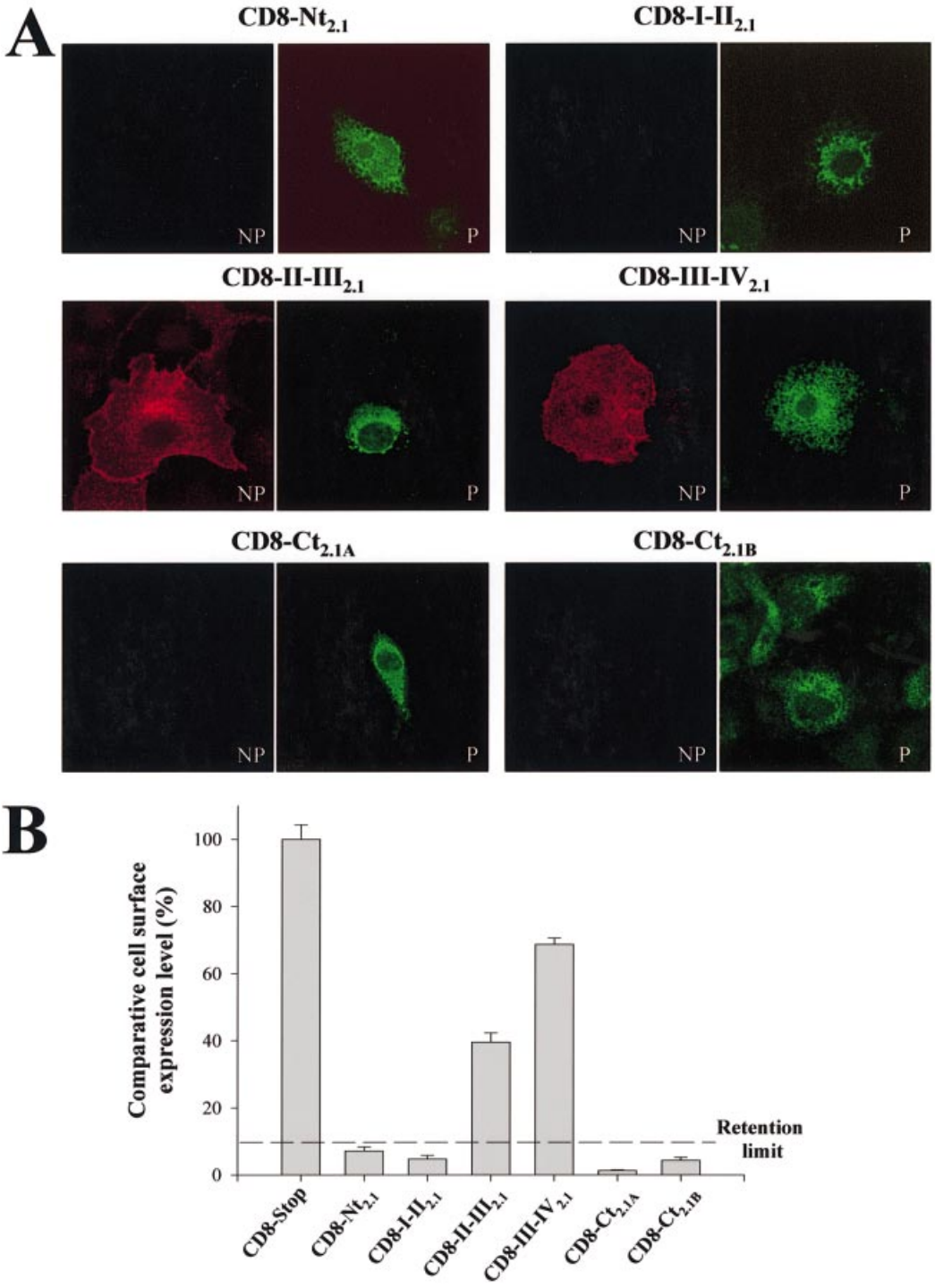

FIG. 3. Cell surface expression efficiency of various CD8-$Ca_v\alpha_{2.1}$ chimeric proteins. (A) The cellular distribution of CD8-$Nt_{2.1}$, CD8-I–$II_{2.1}$, CD8-II–$III_{2.1}$, CD8-III–$IV_{2.1}$, CD8-$Ct_{2.1A}$ and CD8-$Ct_{2.1B}$ chimeric proteins expressed in COS7 cells was observed by confocal microscopy. Non-permeabilized cells were incubated with monoclonal anti-CD8 antibody, followed by detergent permeabilization and incubation with polyclonal anti-CD8 antibodies. Immunostaining was visualized with a GAM-TRITC (membrane staining, NP) and GAR-FITC (intracellular staining, P) antibodies. Whereas CD8-$Nt_{2.1}$ protein was clearly detected following permeabilization, no cell surface expression was visible under nonpermeabilized conditions. Similar results were evident in COS7 cells transfected with CD8-I–$II_{2.1}$, CD8-$Ct_{2.1A}$ and CD8-$Ct_{2.1B}$. For two other chimeras (CD8-II–$III_{2.1}$ and CD8-III–$IV_{2.1}$), large membrane expression was observed in COS7 cells. (B) ELISA quantification of chimera CD8 cell surface expression efficiency in COS7 cells. Membrane expression was normalized to maximal expression of CD8-stop. A retention limit was arbitrarily set three SD values above the SEE value of CD8-I–$II_{2.1}$ (here 7.9%).

maximal achievable SEE level possible (thus 100%), and allowed normalization of all other values obtained to that value (Fig. 3B). Based on this approach, it was confirmed that CD8-$Nt_{2.1}$, CD8-$Ct_{2.1A}$ and CD8-$Ct_{2.1B}$ all have mean SEE values similar to that of CD8-I–$II_{2.1}$ (below the threshold level defined for CD8-I–$II_{2.1}$). On average, CD8-I–$II_{2.1}$ had a 21-fold lower plasma membrane expression efficiency than CD8-stop. CD8-$Nt_{2.1}$, CD8-$Ct_{2.1A}$ and CD8-$Ct_{2.1B}$ all expressed 14-, 79- and 23-fold less well than CD8-stop at the cell surface. In contrast, both CD8-II–$III_{2.1}$ and CD8-III–$IV_{2.1}$ had expression levels well above the threshold level. The SEE values of these two proteins were slightly lower than that of CD8-stop (2.5- and 1.4-fold less than CD8-stop), maybe as a result of inducing a slowing of the export rate of CD8 from the ER.

It has been shown in previous studies that CD8-I–$II_{2.1}$ is not properly expressed at the plasma membrane because of ER retention (Bichet *et al.*, 2000). The aim of this study was therefore to investigate where, along the trafficking pathway, CD8-$Nt_{2.1}$, CD8-$Ct_{2.1A}$ and CD8-$Ct_{2.1B}$, may be retained in the cell. Figure 4 confirms the reticulated intracellular distribution of CD8-I–$II_{2.1}$ and its colocalization with BiP, a resident protein of the ER. A similar localization was observed between the distribution of BiP and CD8-$Nt_{2.1}$ or CD8-$Ct_{2.1A}$ suggesting that these two proteins were also retained in the ER. Also the distribution of CD8-$Ct_{2.1B}$ was related to that of BiP, though the ER-like appearance of the staining was less clear (data not shown). Overall, these findings argue that there are several more retention determinants in $Ca_v\alpha_{2.1}$ beside the I–II loop. It

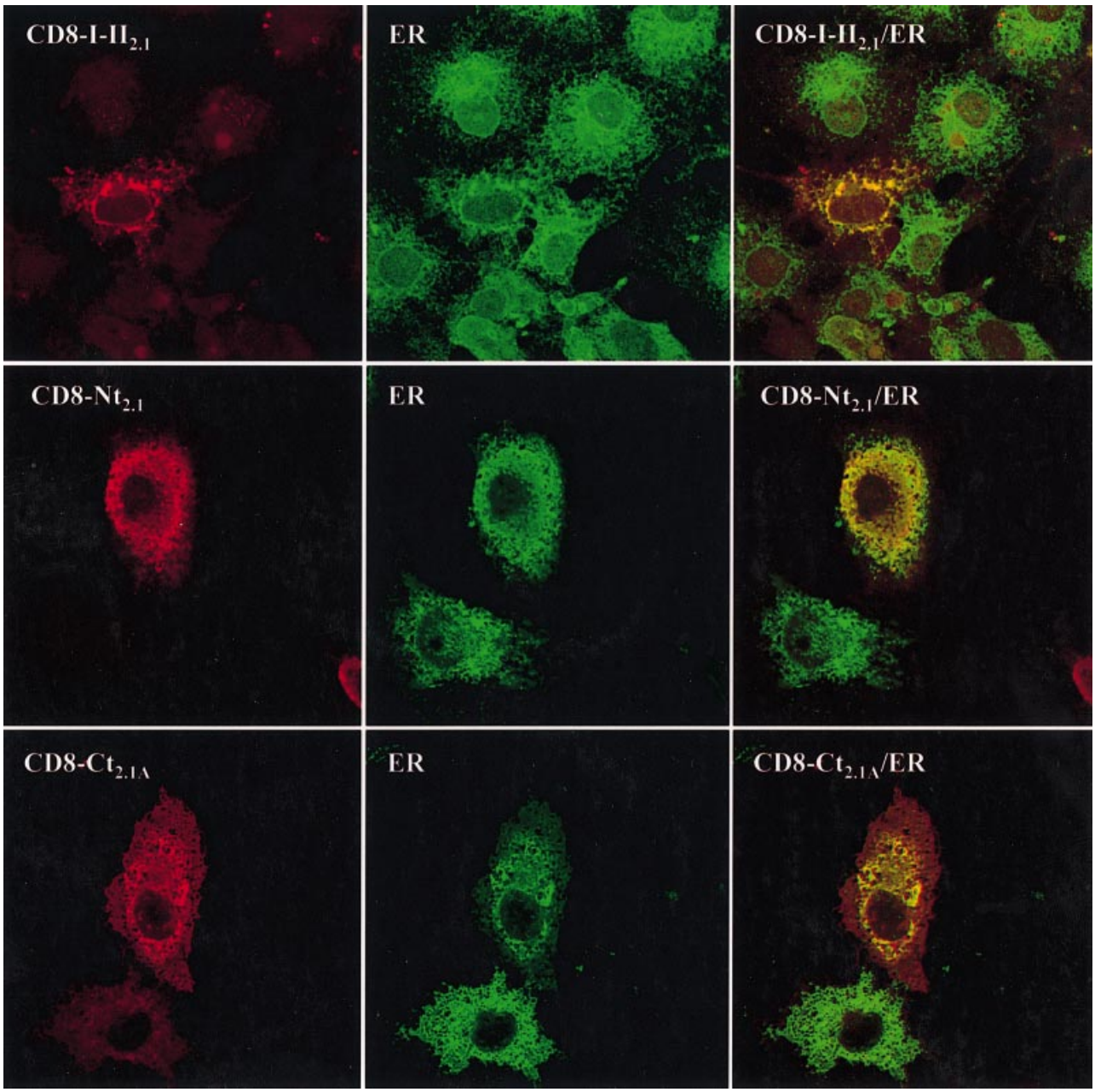

FIG. 4. CD8 chimeric proteins that do not express at the plasma membrane were retained in the ER. The upper panel illustrates a confocal image of the intracellular staining of CD8-I–$II_{2.1}$, the staining of BiP, an ER resident protein, and the colocalization of CD8-I–$II_{2.1}$ with BiP in a permeabilized COS7 cell. The middle and lower panels illustrate similar analyses with CD8-$Nt_{2.1}$ and CD8-$Ct_{2.1A}$, respectively, and come to similar conclusions than with CD8-I–$II_{2.1}$.

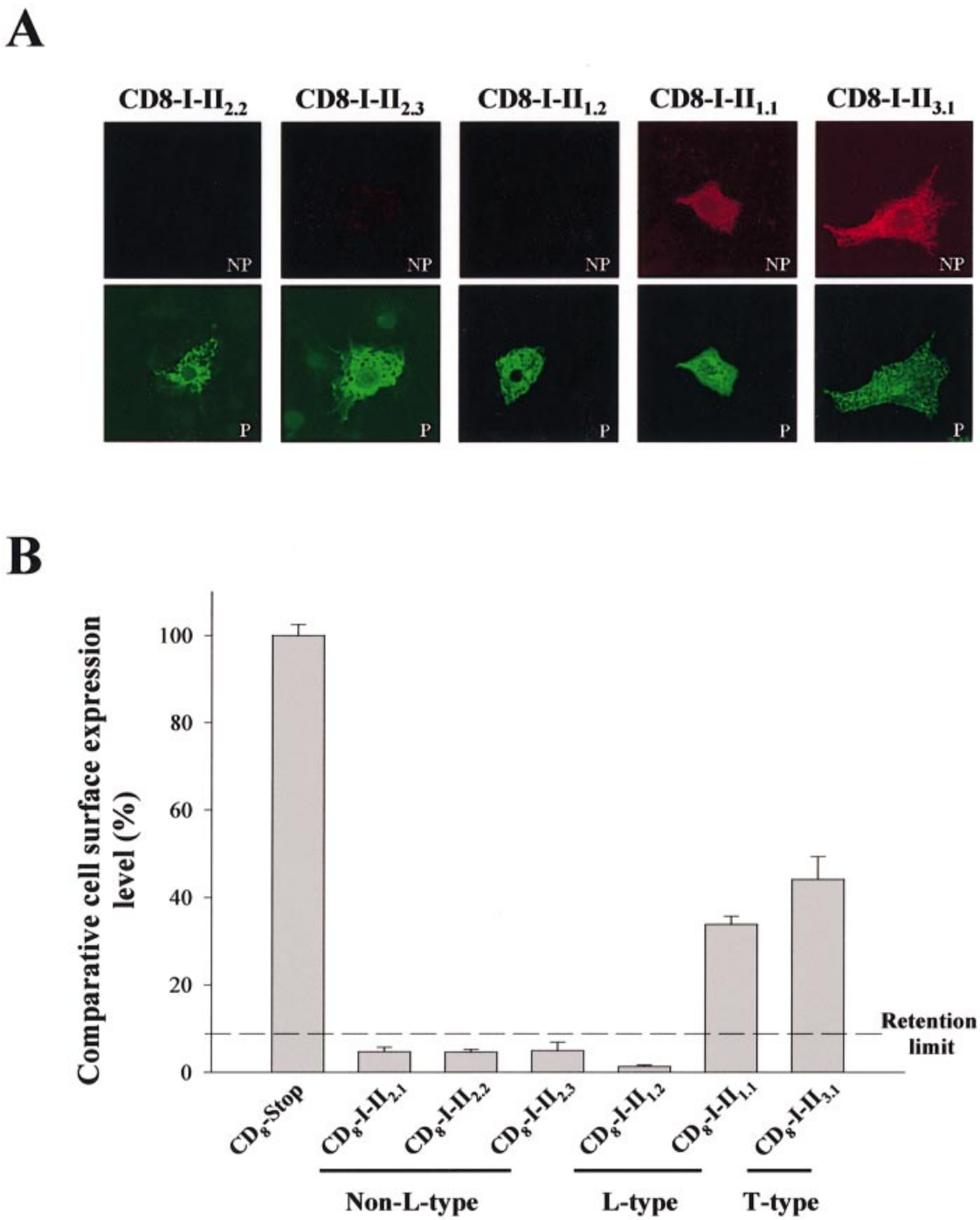

FIG. 5. Comparison of the ER retention of CD8-I–II loop chimeras with different classes of $Ca_v\alpha$ subunits. (A) The immunostaining of various CD8-I–II chimeric proteins was performed as described in Fig. 3. CD8-I–$II_{2.2}$, CD8-I–$II_{2.3}$ and CD8-I–$II_{1.2}$ all expressed poorly at the plasma membrane (non-permeabilized condition, NP) although these proteins were clearly detected in COS7 cells following permeabilization. CD8-I–$II_{1.1}$ was expressed at the plasma membrane of these cells and exhibits a specific punctuate immunostaining. For the T-type chimera (CD8-I–$II_{3.1}$), a clear cell surface expression was evident. (B) ELISA quantification of CD8-I–II chimeric protein cell surface expression efficiency. The retention limit (dashed line) was set at 3 × SD above the mean SEE value for CD8-I–$II_{2.1}$.

was therefore of interest to investigate ER retention in other voltage-dependent calcium channels as well.

First it was investigated whether the possibility that the I–II loop of other $Ca_v\alpha$ isoforms may also possess ER-retention determinants based on the functional homologies, such as $Ca_v\beta$ cell surface expression stimulation, that have been extensively described (for review see Walker & De Waard, 1998). Figure 5A shows the expression of various CD8-$Ca_v\alpha$ chimera proteins in COS7 cells. It was found that the cell distribution of CD8-I–$II_{2.2}$, CD8-I–$II_{2.3}$ and CD8-I–$II_{1.2}$ appeared very similar to that of CD8-I–$II_{2.1}$. It was not

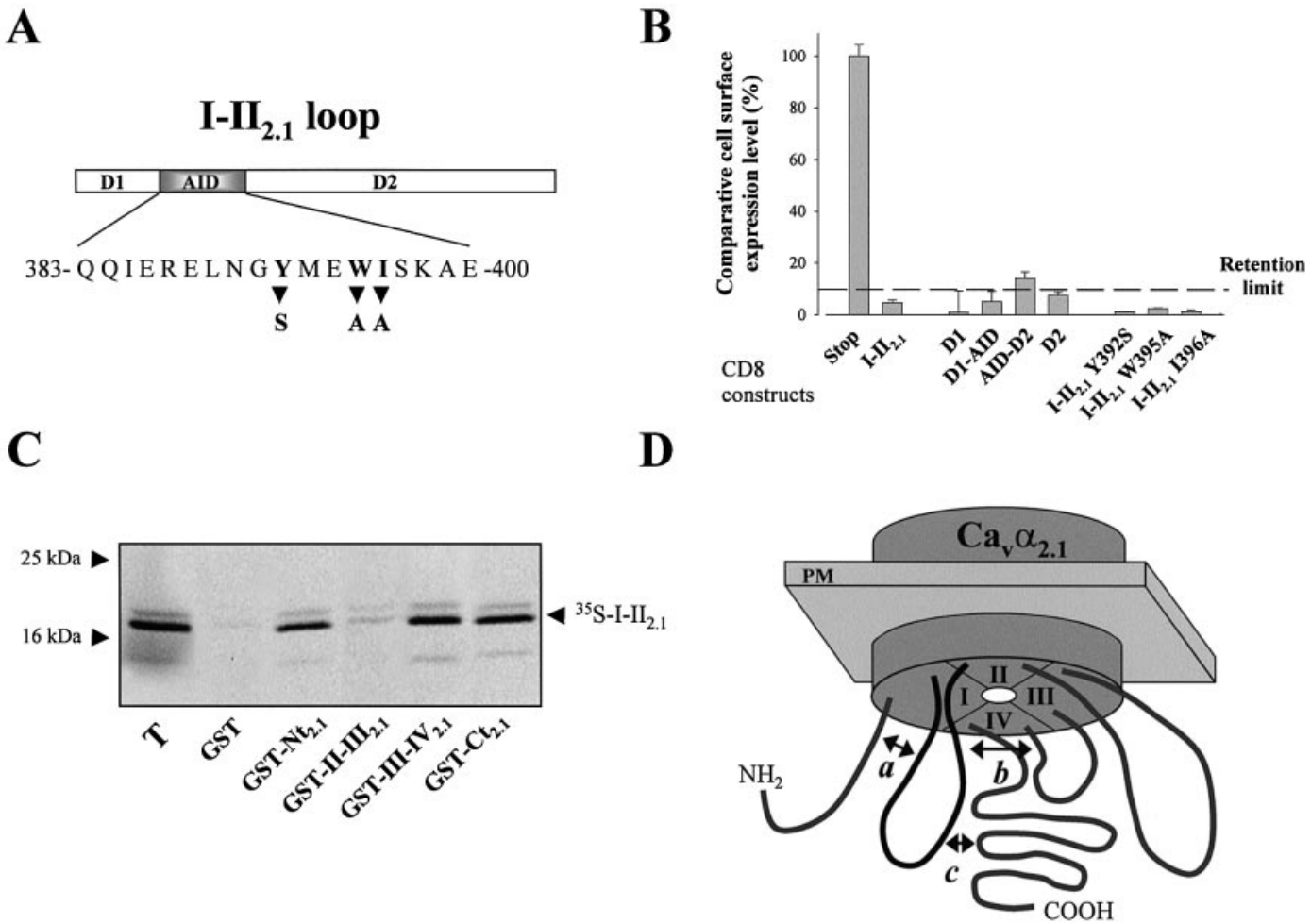

FIG. 6. Multiple ER-retention determinants in the I–II loop of $Ca_v\alpha_{2.1}$ and identification of several novel molecular interactions. (A) Sequence of the AID site of $Ca_v\alpha_{2.1}$ and location of the mutated amino acid residues. The AID sequence corresponds to the primary $Ca_v\beta$ binding site and extends from amino acid 383–400 in $Ca_v\alpha_{2.1}$. The 23 amino acids upstream of AID correspond to domain 1 (D1), whereas the downstream sequence corresponds to domain 2 (D2). Y392, W395 and I396 are three essential residues for $Ca_v\beta$ subunit binding. (B) ELISA quantification of the cell surface expression efficiency of mutated and truncated CD8-I–$II_{2.1}$ proteins. None of the constructs expressed significantly well at the cell surface suggesting that retention determinants in the I–II loop may be disseminated within D1, AID and D2. (C) The full-length I–$II_{2.1}$ loop was translated *in vitro*, labelled with [^{35}S]-methionine, and binding was assayed onto 1 μM of various GST fusion proteins. The [^{35}S]-I–$II_{2.1}$ loop was found to interact with GST-$Nt_{2.1}$, GST-III–$IV_{2.1}$ and GST-$Ct_{2.1}$. No interaction occured with control GST or GST-II–III2$_{.1}$. Overnight autoradiogram exposure time. (D) Schematic diagram illustrating the various intramolecular interactions occurring with the I–II loop. Interaction of the I–II loop: *a*, with the amino-terminus; *b*, with the III–IV loop; and *c*, with the carboxyl-terminus.

possible to clearly visualize cell surface expression of these chimera proteins, but a clear ER-like localization was detectable following cell permeabilization. Surprisingly, it was found that the distribution of CD8-I–$II_{1.1}$ was quite different than that observed for the other CD8-$Ca_v\alpha$ chimeras. The protein is obviously expressed at the cell surface and its distribution appears punctuated suggesting that CD8-I–$II_{1.1}$ may form clusters. This result also suggests that, contrary to other high-voltage-activated calcium channels, ER retention of $Ca_v\alpha_{1.1}$ does not heavily rely on I–II loop determinants. It is therefore possible that ER retention of $Ca_v\alpha_{1.1}$ is based on different cytoplasmic sequences than the I–II loop. Alternatively, the I–II loop of this channel may contribute to $Ca_v\alpha_{1.1}$ ER retention by forming a structural pocket with other essential determinants. To validate the finding that the I–II loop does not necessarily contain an ER-retention determinant, the cell surface expression of CD8-$Ca_v\alpha_{3.1}$ chimera was tested. It was expected that the I–II loop of this member of the low voltage-activated calcium channel family would express well at the plasma membrane, in close agreement with reports that demonstrate in various cell lines the ease with which these channels are expressed in the absence of any auxiliary subunit (Lacinova *et al.*, 2000). Figure 5B illustrates that CD8-I–$II_{3.1}$ is clearly detectable at the plasma membrane. The distribution of CD8-I–$II_{3.1}$ is also punctuated suggesting that it may also form clusters in COS7 cells. The intracellular distribution of this chimera protein is unlike most other CD8-I–II chimeras tested and does not appear to coincide with the ER, suggesting the absence of any ER-retention signal in the I–II loop of $Ca_v\alpha_{3.1}$. These findings were confirmed by determining the SEE values of these chimera proteins (Fig. 5B). Most CD8-I–II chimeras had restricted SEE values coherent with ER retention except for CD8-I–$II_{1.1}$ and CD8-I–$II_{3.1}$ which were well above the threshold for ER retention set by CD8-I–$II_{2.1}$ SEE value. SEE values for CD8-I–$II_{1.1}$ and CD8-I–$II_{3.1}$ were 33.8 ± 1.9% and 44.1 ± 5.2% of CD8-stop, respectively. Again, these values were smaller than those observed for CD8-stop, but similar to those observed for CD8-II–$III_{2.1}$ and CD8-III–$IV_{2.1}$. The clustering behaviour of these proteins may explain these small differences in SEE levels with that of CD8-stop.

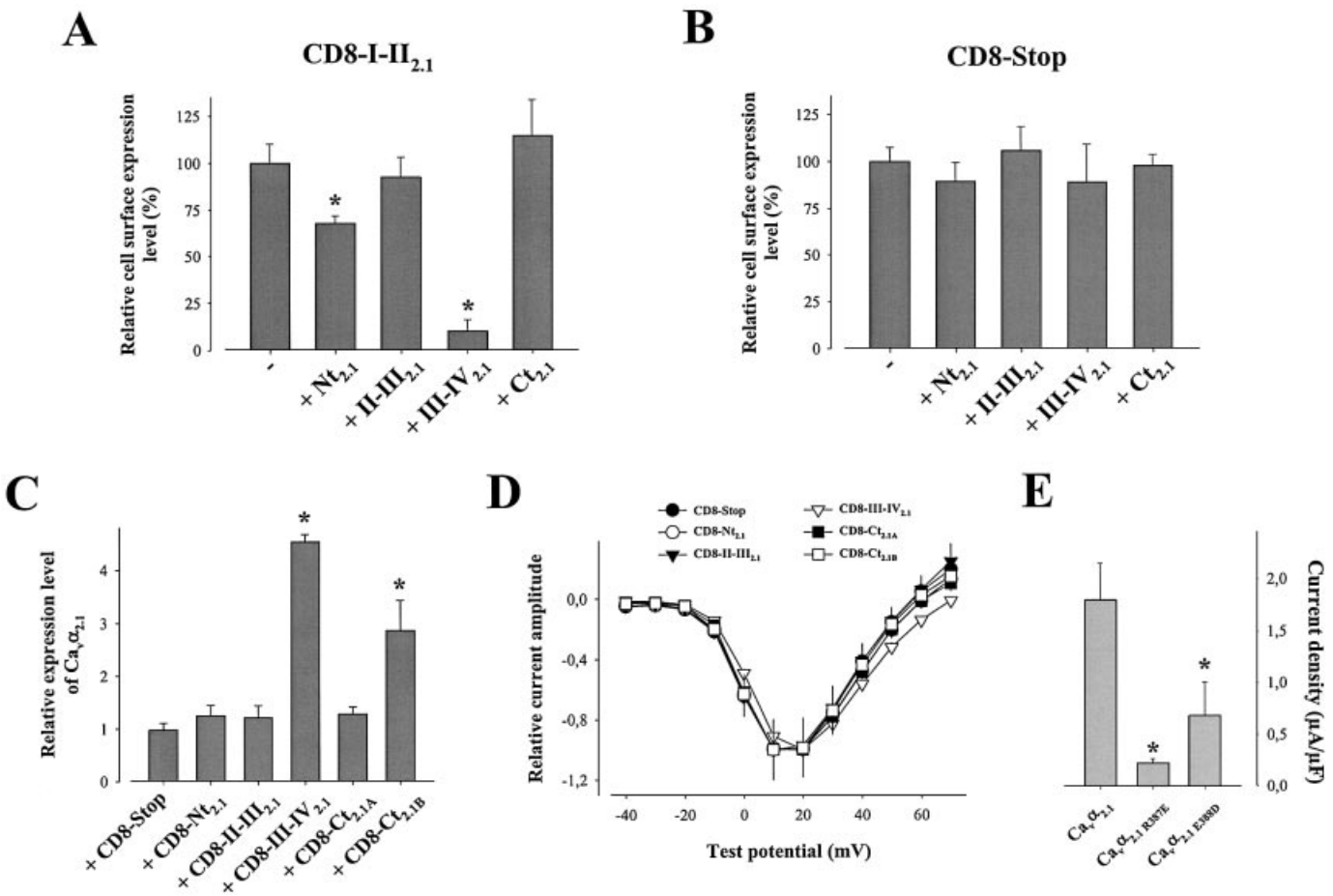

FIG. 7. Internal molecular interactions of the I–II loop influenced cell surface expression of $Ca_vα_{2.1}$ expressed in *xenopus* oocytes. (A) The effect of $Ca_vα_{2.1}$ cytoplasmic fragment expression was assessed on the SEE level of CD8-I–$II_{2.1}$. Both the N-terminus and the III–IV loop further inhibited the cell surface expression level of CD8-I–$II_{2.1}$. (B) Same as (A) but with control CD8-stop. None of the $Ca_vα_{2.1}$ fragments influenced CD8-stop cell surface expression efficiency. (C) The current densities of $Ca_vα_{2.1}$ expressed in *xenopus* oocytes were normalized to the value obtained for $Ca_vα_{2.1}$ expression with CD8-stop. Test potential was 20 mV and holding potential –90 mV. Both CD8-III–$IV_{2.1}$ and CD8-$Ct_{2.1B}$ improved the expression of $Ca_vα_{2.1}$. (D) Current-voltage relationship of $Ca_vα_{2.1}$ expressed with either CD8-stop or CD8-$Ca_vα_{2.1}$ chimera constructs. (E) Average current densities of wild-type $Ca_vα_{2.1}$ (n = 9) and mutant $Ca_vα_{2.1}$ R387E (n = 10) and $Ca_vα_{2.1}$ E388D (n = 7) channels expressed in *xenopus* oocytes. Test potential was 20 mV and holding potential –90 mV.

Evidence has been presented that deletions with the I–II loop may partially facilitate the cell surface expression of $Ca_vα_{2.1}$ in *xenopus* oocytes (Bichet *et al.*, 2000). Deleting important amino acid regions of the channel may effectively remove ER-retention determinants, but, conversely, presents the drawback that it can destabilize the overall structure and function of the channel. Indeed, small I–II loop deletions could facilitate cell surface channel expression, but larger deletions either rendered the channel inactive or improved ER retention (Bichet *et al.*, 2000). As partial deletions of the alpha1 interaction domain (AID) of the subunit were effective in antagonizing ER retention, it is possible that one of the ER-retention determinants in $Ca_vα_{2.1}$ coincides with the domain required for $Ca_vβ$ subunit association. For this reason, it was examined whether point mutations in the I–II loop would facilitate the SEE values of the chimeric CD8-I–$II_{2.1}$ protein (Fig. 6A and B). The mutations performed in CD8-I–$II_{2.1}$ (Y392S, W395A and I396A) were those that prevent the normal association of the $Ca_vβ$ subunit to $Ca_vα_{2.1}$ (De Waard *et al.*, 1996). Figure 6B illustrates that none of the mutated CD8-I–$II_{2.1}$ proteins had SEE values higher than the wild-type CD8-I–$II_{2.1}$ protein suggesting that ER retention of the I–II loop does not rely on these residues, or at least not exclusively. A number of further deletions were performed in the I–II loop to consider whether deletion or expression of the domains (D1, amino-acids 360–382, and D2, amino acids 401–487 of $Ca_vα_{2.1}$) preceding or following the AID site were important in retention. The data illustrates that protein retention cannot be reduced to a single domain of the I–II loop. On the contrary, most of the I–II loop sequence contributes to retention, presumably through multiple and discrete determinants. As, however, it is clearly established that $Ca_vβ$ subunit expression facilitates cell surface expression of the channel through interaction with a single region of the I–II loop, the AID site, one has to envision that other retention determinants within the channel are presumably masked through a different set of protein interactions than the sole $Ca_vα/Ca_vβ$ interaction. Figure 6C demonstrates that *in vitro* translated [^{35}S]-I–$II_{2.1}$ loop is able to interact with GST fusion proteins containing the III–$IV_{2.1}$ loop, the amino- and carboxy-termini of $Ca_vα_{2.1}$, but not GST alone or GST-II–$III_{2.1}$. This observation suggests that the I–II loop forms a ternary interaction complex with various internal sequences of $Ca_vα_{2.1}$ as summarized in Fig. 6D. The concept of intramolecular interaction sites is not novel as it is also known to occur in voltage-dependent Na^+ channels (Zhang *et al.*, 2000).

One may speculate that these internal $Ca_v\alpha_{2.1}$ interactions could mask some of the ER-retention determinants identified with the I–II loop and the N- and C-termini. To test this hypothesis, the effects of various cytoplasmic fragments of $Ca_v\alpha_{2.1}$ on CD8-I–$II_{2.1}$ cell surface expression levels were analysed (Fig. 7A). *Xenopus* oocytes were used for this study to allow a comparison with the functional effects of these fragments on the full-length $Ca_v\alpha_{2.1}$ expressed in these cells. It was found that, amongst the cytoplasmic sequences known to interact with the I–II loop (Fig. 6C and D), only the amino-terminus and the III–$IV_{2.1}$ loop, influence the SEE values of the CD8-I–$II_{2.1}$ chimera. The $Nt_{2.1}$ fragment and the III–$IV_{2.1}$ loop decreased CD8-I–$II_{2.1}$ SEE values by a factor of 1.5- and 16.2-fold, respectively. In contrast, none of these fragments had any effect on the SEE level of the CD8-stop protein, taken as a control, thereby illustrating the specificity of these effects (Fig. 7B). As the CD8-I–$II_{2.1}$ chimera cannot solely stand for the structural complexity of the full-length $Ca_v\alpha_{2.1}$ channel, the absolute effect of these fragments on the SEE level of CD8-I–$II_{2.1}$ should not be extrapolated to the channel itself. However, this data is a strong indication that these sequences potentially possess an important modulating function. Thus, the next step was to assess the effect of over-expression of CD8 chimeras on $Ca_v\alpha_{2.1}$ expression level in *xenopus* oocytes. The choice of this expression system over COS7 cells is justified by the fact that COS7 cells are unable to express reliable and reproducible $Ca_v\alpha_{2.1}$ calcium currents when the channel is expressed in the absence of auxiliary subunits. Current densities measured at 20 mV can be taken as an index of cell surface expression level. The results, summarized in Fig. 7C, demonstrate that control CD8-stop, along with several other chimeric proteins (CD8-$Nt_{2.1}$, CD8-II–$III_{2.1}$ and CD8-$Ct_{2.1A}$), has no effect on $Ca_v\alpha_{2.1}$ current densities. However, both CD8-III–$IV_{2.1}$ and CD8-$Ct_{2.1B}$ were found to significantly improve the expression level of $Ca_v\alpha_{2.1}$. The stimulation factors observed on current densities were 4.5 and 2.9-fold for CD8-III–$IV_{2.1}$ and CD8-$Ct_{2.1B}$, respectively. Current stimulations were not due to a displacement in the voltage-dependence of activation as activation curves were strictly similar in the various experimental conditions (Fig. 7D). Half-activation potentials were all in the range of 1.2–3.7 mV, the two extreme values observed. Curiously, $Ca_v\alpha_{2.1}$ channel fragments (e.g. III–IV loop) sometimes produced effects on current densities that could be different from those observed on CD8-I–$II_{2.1}$ SEE levels. This observation is not so shocking as the CD8-I–II chimera does not integrate the structural and regulatory complexity of the I–II loop in its native $Ca_v\alpha$ environment. On a speculative basis, it can be imagined that binding of the III–IV loop onto CD8-I–II reinforces ER retention by better exposing other ER-retention determinants present within the I–II sequence, whereas, owing to the multiple other interactions and regulation that take place on this loop in its native environment, it does not act similarly on the full length channel, where it would rather mask the last available ER-retention determinants. The data obtained by coexpressing channel fragments with $Ca_v\alpha_{2.1}$ demonstrate that internal protein interactions can dramatically affect the cell surface expression efficiency of $Ca_v\alpha_{2.1}$. As an explanation of these effects, it was assumed that these interactions may mask one or many ER-retention sites of $Ca_v\alpha_{2.1}$, thereby facilitating the cell trafficking of the channel. This hypothesis is reinforced by the observation that $Ca_v\alpha_{2.1}$ sequences (such as the II–III loop), that do not interact with the I–II loop, also have no effect on channel expression. The effect of the III–IV loop on $Ca_v\alpha_{2.1}$ expression prompted further confirmatory experiments on the role of this loop in ER retention. It has recently been demonstrated that the binding of a $Ca_v\beta$ subunit onto AID modifies $Ca_v\alpha_{2.1}$ inactivation by inhibiting the interaction between the I–II and III–IV loops (Fathallah *et al.*, 2002; Geib *et al.*, 2002). This effect of $Ca_v\beta$ on the I–II/III–IV loop interaction can be mimicked by point mutation of either R387 or E388 present as non-conserved amino acid residues within the AID sequence of the I–II loop (Geib *et al.*, 2002). One can therefore envision that if this I–II/III–IV loop interaction is important in ER retention, as expected from the III–IV loop over-expression, then R387 or E388 mutant $Ca_v\alpha_{2.1}$ channels should have altered the cell surface expression of the channel. Figure 7E does indeed demonstrate that the current densities of both $Ca_v\alpha_{2.1}$ channel mutants (R387E and E388D) were reduced by 88 and 62%, respectively. These data suggest again that the interaction of the III–IV loop with the I–II loop favours the cell surface expression of the channel.

Discussion

Cell surface expression of voltage-dependent calcium channels is a highly regulated process. Several inhibitory mechanisms take place to avoid excessive calcium entry through the plasma membrane. Concomitantly, one would expect that multiple molecular determinants control the spatial distribution of voltage-dependent calcium channel structures at the cell surface in a functionally deterministic manner (e.g. synaptic localization for P/Q channels implicated in neurotransmitter release). For these reasons, a better understanding of the mechanisms that control calcium channel expression level and plasma membrane distribution is required.

In this study, a quantitative approach has been used to demonstrate that the I–II loop of $Ca_v\alpha_{2.1}$ contains multiple ER-retention determinants. This observation was also extended to several other high-threshold calcium channels. However, the cell surface quantification assay also demonstrates that, besides the I–II loop, both the amino- and carboxyl-termini of $Ca_v\alpha_{2.1}$ are also involved in ER retention. There are several other examples in which the carboxyl terminal sequence is involved in ER retention (McIlhinney *et al.*, 1998; Zerangue *et al.*, 1999). It is for instance the primary locus for ER retention of the $GABA_{B1}$ subunit of the metabotropic $GABA_B$ receptor (Margeta-Mitrovic *et al.*, 2000). The cytoplasmic localization of ER-retention determinants is not so surprising as several other proteins, such as the adenovirus E19 glycoprotein (Paabo *et al.*, 1987), are retained in the ER through cytoplasmic domains. Although this observation points to several different cytoplasmic loci in the primary structure of the channel, this does not necessarily imply that there are as many ER-retention determinants in correctly folded $Ca_v\alpha_{2.1}$ channels than the ones identified by the CD8 chimera approach. In fact, this study presents evidence that the I–II loop of $Ca_v\alpha_{2.1}$ may form a larger structural ER-retention zone through the interaction with the N- and C-termini of the channel. Besides, it also known that these three regions all bind to the auxiliary $Ca_v\beta_4$ subunit in P/Q channels (Walker *et al.*, 1998, 1999), suggesting that they should form a single $Ca_v\beta$ binding pocket. Similarly, these data are also in agreement with the findings that the regulatory $G\beta\gamma$ complex is able to bind all three structural elements: the I–II loop (De Waard *et al.*, 1997), the N-terminus (Stephens *et al.*, 1998; Canti *et al.*, 1999) and the C-terminus (Qin *et al.*, 1997). Thus, results demonstrating that the I–II loop is in interaction with several other cytoplasmic sequences of $Ca_v\alpha_{2.1}$ are in line with the concept that the ER-retention determinants cannot simply be assimilated to linear structures.

It should be emphasized that the 3-D complexity, resulting from the association of one or several other cytoplasmic sequences with the I–II loop, does not necessarily imply the formation of a global ER-retention zone made of the addition of individual determinants.

According to other examples in the literature, it is more attractive to believe that the proper folding of $Ca_v\alpha_{2.1}$, a process by which an organized pattern of internal interactions would take place, results in a numerical simplification of the ER-retention determinants. The concept whereby ER-retention determinants are masked by protein interactions is not novel as, for instance, the ER-retention signal present in the C-terminus of the $GABA_{B1b}$ subunit is masked by its interaction with the C-terminus of the $GABA_{B2}$ subunit (Margeta-Mitrovic *et al.*, 2000). NR1, an ionotropic NMDA receptor subunit, is also retained in the ER in the absence of NR2 (McIlhinney *et al.*, 1998). Thus, a progressive masking of ER-retention signals during folding of $Ca_v\alpha_{2.1}$ also appears to be an attractive mechanism for the facilitated export of the channel out of the ER. The data described here point to the importance of internal molecular interactions for an efficient export of the channel, as over-expression of some interacting domains (III–IV loop and C-terminus) facilitate channel expression (Fig. 7C). It is interesting to note that, in the case of the III–IV loop, this facilitation is induced by a sequence that is not itself implicated in ER retention. Interestingly, this III–IV loop has been shown to bind onto the I–II loop through N-terminal residues of the AID site (Geib *et al.*, 2002). One attractive hypothesis is that the III–IV loop facilitates the expression of $Ca_v\alpha_{2.1}$ through mechanisms that are partially shared by the $Ca_v\beta$ subunit, also known for its ability to bind onto AID. The observation that the cell surface expression efficiency of CD8-I–$II_{2.1}$ does not behave similarly to the full-length $Ca_v\alpha_{2.1}$ in the presence of each cytoplasmic $Ca_v\alpha_{2.1}$ fragment argues that the correct molecular environment of the I–II loop greatly influences the efficiency of its ER export. Further, it strongly argues that correct folding is an essential step to prepare the channel for $Ca_v\beta$ subunit association and subsequent ER export. On a more methodological note, the differences observed in cell surface expression efficiency between full-length $Ca_v\alpha_{2.1}$ and CD8 chimeras point to analytical restrictions inherent to the chimera approach. The CD8 chimeric proteins are clearly useful for discovering ER-retention signals but are less interesting for defining anti-retention strategies. This was obvious from the expression of CD8 chimeras with I–II loop mutations or deletions whose cell surface expression efficiencies were not improved contrary to some deletions in the I–II loop of the full length $Ca_v\alpha_{2.1}$ channel (Bichet *et al.*, 2000). Thus, anti-retention strategies need to be developed for the full-length channel that better integrates the structural and regulatory complexities of the sequences under study.

Although the concept of ER-retention site masking has been proven on experimental grounds, it is however, very difficult to precisely depict the exact location and function of each ER-retention determinant on $Ca_v\alpha_{2.1}$ and how these determinants are masked. For instance, the ER-retention determinants appear quite disseminated throughout the I–II loop sequence as sequence deletion within the CD8-I–$II_{2.1}$ chimera had little impact on ER retention. The multiplicity of ER-retention determinants has however, several interesting implications. ER-retention determinant masking and unmasking may represent an important regulatory function or the basis for a pathophysiological state of the channel. There are two simple illustrations of this statement. Firstly, it is obvious that the ER-retention determinant masking ability of the $Ca_v\beta_4$ subunit, which binds onto both the N- and C-termini of $Ca_v\alpha_{2.1}$ (Walker *et al.*, 1998, 1999), in addition to AID (Pragnell *et al.*, 1994), should be superior to that of the $Ca_v\beta_3$ subunit. Indeed, the $Ca_v\beta_3$ subunit is unable to bind to any other structure than the I–II loop, leaving open the possibility that the N- and C-termini of $Ca_v\alpha_{2.1}$ continue to act in favour of ER retention in the absence of any other protein interaction. This is indeed the case according to a recent study, with a 2.5-fold greater $Ca_v\alpha_{2.1}$ expression stimulation efficiency for $Ca_v\beta_4$ over $Ca_v\beta_3$ subunit (Sandoz *et al.*, 2001). Secondly, unmasking of I–II loop ER-retention signals through structural reorganization of the carboxyl-terminus of $Ca_v\alpha_{2.1}$ could be an interesting molecular mechanism for inducing abnormal calcium channel function. In this respect, it would thus be of interest to investigate the properties of ER retention of $Ca_v\alpha_{2.1}$ channels affected by leaner, or SCA6, mutations. In the study of Bichet *et al.* (2000), it was indeed demonstrated that sequence deletion within the full length $Ca_v\alpha_{2.1}$ channel could effectively facilitate its cell surface expression. However, extensive deletions had the opposite effect, possibly because some ER-retention site unmasking may have occurred in these constructs. Pathologic mutation/deletion can also result in ER maintenance, for example the CFTR chloride channel (Gilbert *et al.*, 1998). It should be emphasized that the issue remains inherently complex because, besides the 'negative retention signals', there are also 'positive export signals' involved in calcium channel trafficking and incorporation into the plasma membrane, very much like those identified in potassium channels (Ma *et al.*, 2001). The proper localization of $Ca_v\alpha_{1.1}$ to the triad junction of skeletal muscle, for instance, is induced by the last 55 amino acid residues of this subunit (Flucher *et al.*, 2000). Similarly, a C-terminal sequence of $Ca_v\alpha_{1.2}$ (amino acid residues 1623–1666) has been implicated in $Ca_v\beta$-independent plasma membrane expression (Gao *et al.*, 2000).

It was of interest in this study to investigate whether all $Ca_v\alpha$ channels were equivalent with regard to ER retention. Similarities were expected on the basis that $Ca_v\beta$ subunits have tremendous effects on the cell surface expression level of all high voltage-gated calcium channels (Walker & De Waard, 1998). In contrast, low voltage-gated calcium channels express at high levels in the absence of $Ca_v\beta$ subunits. In agreement with the former observation, it was found that CD8-I–$II_{3.1}$ chimeric protein expressed at normal levels at the cell surface whereas most other CD8-I–II chimeras derived from the $Ca_v\alpha_1$ and $Ca_v\alpha_2$ classes were expressed little or not at all. There is a singular exception to this rule as CD8-I–$II_{1.1}$ was found to express quite well in COS7 cells in the absence of a $Ca_v\beta$ subunit. It is thus possible that ER-retention signals are distributed differently from one $Ca_v\alpha$ channel to the another. Amongst the residues identified in the I–II loop of $Ca_v\alpha_{2.1}$, including several double arginine motifs (Schutze *et al.*, 1994), only a few are really conserved in $Ca_v\alpha_{1.1}$ suggesting that the distribution of ER-retention determinants varies greatly. This observation does, however, raise the question of how the $Ca_v\beta$ subunit may proceed to enhance the cell surface expression of $Ca_v\alpha_{1.1}$. The suspicion is therefore that, upon binding to the I–II loop, it may act by producing as strong rearrangements in the channel structure as those that appear to have been uncovered for $Ca_v\alpha_{2.1}$. Alternatively, the I–II loop of $Ca_v\alpha_{1.1}$ may form a complex structural ER-retention pocket only through the interaction with other loops. Yet another possibility is that, clustering of the molecule, which is observed to occur for this isoform only, may prevent normal retention taking place. At this stage, it can only be speculated that such a variation is meant to help the regulation of the trafficking of these channels to the plasma membrane. Such behaviour is expected on the basis that different calcium channels have different fates and cell surface destination in agreement with the cellular functions they have to fulfill.

In conclusion, these data indicate that $Ca_v\alpha_{2.1}$ probably auto-proceeds to the masking of several potential ER-retention signals assuring that only correctly folded molecules will be taken in charge by the $Ca_v\beta$ subunit. One has therefore to envision the $Ca_v\beta$ subunit as a final unlocking key, but only for correctly processed $Ca_v\alpha$ subunits.

References

Bichet, D., Cornet, V., Geib, S., Carlier, E., Volsen, S., Hoshi, T., Mori, Y. & De Waard, M. (2000) The I–II loop of the Ca^{2+} channel α_1 subunit contains an endoplasmic reticulum retention signal antagonized by the β subunit. *Neuron*, **25**, 177–190.

Brice, N.L., Berrow, N.S., Campbell, V., Page, K.M., Brickley, K., Tedder, I. & Dolphin, A.C. (1997) Importance of the different beta subunits in the membrane expression of the alpha1A and alpha2 calcium channel subunits: studies using a depolarization-sensitive alpha1A antibody. *Eur. J. Neurosci.*, **9**, 749–759.

Canti, C., Page, K.M., Stephens, G.J. & Dolphin, A.C. (1999) Identification of residues in the N terminus of α1B critical for inhibition of the voltage-dependent calcium channel by Gβγ. *J. Neurosci.*, **19**, 6855–6864.

Davare, M.A., Avdonin, V., Hall, D.D., Peden, E.M., Burette, A., Weinberg, R.J., Horne, M.C., Hoshi, T. & Hell, J.W. (2001) A beta2 adrenergic receptor signaling complex assembled with the Ca^{2+} channel $Ca_v1.2$. *Science*, **293**, 98–101.

De Waard, M., Liu, H., Walker, D., Scott, V.E., Gurnett, C. & Campbell, K.P. (1997) Direct binding of G-protein betagamma complex to voltage-dependent calcium channels. *Nature*, **285**, 446–450.

De Waard, M., Scott, V.E., Pragnell, M. & Campbell, K.P. (1996) Identification of critical amino acids involved in alpha1–beta interaction in voltage-dependent Ca^{2+} channels. *FEBS Lett.*, **380**, 272–276.

De Waard, M., Witcher, D.R., Pragnell, M., Liu, H. & Campbell, K.P. (1995) Properties of the α_1-β anchoring site in voltage-dependent Ca^{2+} channels. *J. Biol. Chem.*, **270**, 12056–12064.

Eppig, J.J. & Dumont, J.N. (1976) Defined nutrient medium for the *in vitro* maintenance of *Xenopus* laevis oocytes. *In Vitro*, **12**, 418–427.

Ertel, E.A., Campbell, K.P., Harpold, M.M., Hofmann, F., Mori, Y., Perez-Reyes, E., Schwartz, A., Snutch, T.P., Tanabe, T., Birnbaumer, L., Tsien, R.W. & Catterall, W.A. (2000) Nomenclature of voltage-gated calcium channels. *Neuron*, **25**, 533–535.

Fathallah, M., Sandoz, G., Mabrouk, K., Geib, S., Urbani, J., Villaz, M., Ronjat, M. Sabatier, J.M. & De Waard, M. (2002) Modelling of the III-IV loop, a domain involved in calcium channel Ca(v)2.1 inactivation, highlights a structural homology with the gamma subunit of G proteins. *Eur. J. Neurosci.*, **16**, 219–228.

Flockerzi, V., Oeken, H.-J., Hofmann, F., Pelzer, D., Cavalie, A. & Trautwein, W. (1986) Purified dihydropyridine-binding site from skeletal muscle t-tubule is a functional calcium channel. *Nature*, **323**, 66–68.

Flucher, B.E., Kasielke, N. & Grabner, M. (2000) The triad targeting signal of the skeletal muscle calcium channel is localized in the COOH terminus of the alpha (1S) subunit. *J. Cell Biol.*, **151**, 467–478.

Gao, T., Bunemann, M., Gerhardstein, B.L., Ma, H. & Hosey, M.M. (2000) Role of the C terminus of the alpha 1C ($Ca_v1.2$) subunit in membrane targeting of cardiac 1-type calcium channels. *J. Biol. Chem.*, **275**, 25436–25444.

Geib, S., Sandoz, G., Cornet, V., Mabrouk, K., Fund-Saunier, O., Bichet, D., Villaz, M., Hoshi, T., Sabatier, J.M. & De Waard, M. (2002) The interaction between the I–II loop and the III–IV loop of $Ca_v2.1$ contributes to voltage-dependent inactivation in a β-dependent manner. *J. Biol. Chem.*, **277**, 10003–10013.

Gilbert, A., Jadot, M., Leontieva, E., Wattiaux-De Coninck, S. & Wattiaux, R. (1998) Delta F508 CFTR localizes in the endoplasmic reticulum-Golgi intermediate compartment in cystic fibrosis cells. *Exp Cell Res.*, **242**, 144–152.

Lacinova, L., Klugbauer, N. & Hofmann, F. (2000) Low voltage activated calcium channels: from genes to function. *General Physiol. Biophys.*, **19**, 121–136.

Liu, H., De Waard, M., Scott, V.E.S., Gurnett, C.A., Lennon, V.A. & Campbell, K.P. (1996) Identification of three subunits of the high affinity ω-conotoxin MVIIC-sensitive Ca^{2+} channel. *J. Biol. Chem.*, **271**, 13804–13810.

Ma, D., Zerangue, N., Lin, Y.F. & Collins, A., YuM., Jan, Y.N. & Jan, L.Y. (2001) Role of ER Export Signals in Controlling Surface Potassium Channel Numbers. *Science*, **291**, 316–319.

Margeta-Mitrovic, M., Jan, Y.N. & Jan, L.Y. (2000) A trafficking checkpoint controls GABA (B) receptor heterodimerization. *Neuron*, **27**, 97–106.

McIlhinney, R.A., Le Bourdelles, B., Molnar, E., Tricaud, N., Streit, P. & Whiting, P.J. (1998) Assembly intracellular targeting and cell surface expression of the human N-methyl-D-aspartate receptor subunits NR1A and NR2A in transfected cells. *Neuropharmacology*, **37**, 1355–1367.

Mori, Y., Friedrich, T., Kim, M.S., Mikami, A., Nakai, J., Ruth, P., Bosse, E., Hofmann, F., Flockerzi, V., Furuichi, T., Mikoshiba, K., Imoto, K., Tanabe, T. & Numa, S. (1991) Primary structure and functional expression from complementary DNA of a brain calcium channel. *Nature*, **350**, 398–402.

Paabo, S., Bhat, B.M., Wold, W.S.M. & Peterson, P.A. (1987) A short sequence in the COOH-terminus makes an adenovirus membrane glycoprotein a resident of the endoplasmic reticulum. *Cell*, **50**, 311–317.

Pragnell, M., De Waard, M., Mori, Y., Tanabe, T., Snutch, T.P. & Campbell, K.P. (1994) Calcium channel β-subunit binds to a conserved motif in the I–II cytoplasmic linker of the α_1-subunit. *Nature*, **368**, 67–70.

Qin, N., Platano, D., Olcese, R., Stefani, E. & Birnbaumer, L. (1997) Direct interaction of Gβγ with a C-terminal Gβγ-binding domain of the Ca^{2+} channel alpha1 subunit is responsible for channel inhibition by G protein-coupled receptors. *Proc. Natl. Acad. Sci. USA*, **94**, 8866–8871.

Reimer, D., Huber, I.G., Garcia, M.L., Haase, H. & Striessnig, J. (2000) β subunit heterogeneity of 1-type Ca^{2+} channels in smooth muscle tissues. *FEBS Lett.*, **467**, 65–69.

Sandoz, G., Bichet, D., Mori, Y., Felix, R. & De Waard, M. (2001) Distinct properties and differential β subunit regulation of two C-terminal isoforms of the P/Q-type Ca^{2+}-channel α_{1A} subunit. *Eur. J. Neurosci.*, **14**, 987–997.

Schutze, M.P., Peterson, P.A. & Jackson, M.R. (1994) An N-terminal double-arginine motif maintains type II membrane proteins in the endoplasmic reticulum. *EMBO J.*, **13**, 1696–1705.

Scott, V.E.S., De Waard, M., Liu, H., Gurnett, C.A., Venzke, D.P., Lennon, V.A. & Campbell, K.P. (1996) β subunit heterogeneity in N-type Ca^{2+} channels. *J. Biol. Chem.*, **271**, 3207–3212.

Stephens, G.J., Canti, C., Page, K.M. & Dolphin, A.C. (1998) Role of domain I of neuronal Ca2+ channel alpha1 subunits in G protein modulation. *J. Physiol. (Lond.)*, **509**, 163–169.

Sutton, K.G., McRory, J.E., Guthrie, H., Murphy, T.H. & Snutch, T.P. (1999) P/Q-type calcium channels mediate the activity-dependent feedback of syntaxin-1A. *Nature*, **401**, 800–804.

Walker, D., Bichet, D., Campbell, K.P. & De Waard, M. (1998) A beta 4 isoform–specific interaction site in the carboxyl-terminal region of the voltage-dependent Ca^{2+} channel alpha1A subunit. *J. Biol. Chem.*, **273**, 2361–2367.

Walker, D., Bichet, D., Geib, S., Mori, E., Cornet, V., Snutch, T.P., Mori, Y. & De Waard, M. (1999) A new beta subtype–specific interaction in alpha1A subunit controls P/Q-type Ca^{2+} channel activation. *J. Biol. Chem.*, **274**, 12383–12390.

Walker, D. & De Waard, M. (1998) Subunit interaction sites in voltage-dependent Ca^{2+} channels: role in channel function. *Trends Neurosci.*, **21**, 148–154.

Witcher, D.R., De Waard, M., Sakamoto, J., Franzini-Armstrong, C., Pragnell, M., Kahl, S.D. & Campbell, K.P. (1993) Subunit identification and reconstitution of the N-type Ca^{2+} channel complex purified from brain. *Science*, **261**, 486–489.

Zerangue, N., Schwappach, B., Jan, Y.N. & Jan, L.Y. (1999) A new ER trafficking signal regulates the subunit stoichiometry of plasma membrane K (ATP) channels. *Neuron*, **22**, 537–548.

Zhang, H., Kolibal, S., Vanderkooi, J.M., Cohen, S.A. & Kallen, R.G. (2000) A carboxy-terminal α-helical segment in the rat skeletal muscle voltage-dependent Na^+ channel is responsible for its interaction with the amino-terminus. *Biochim. Biophys. Acta*, **1467**, 406–418.